from the region where it was formerly abundant.

The sun star is a top carnivore in the rocky intertidal zone and may play an important role in structuring intertidal communities in the Gulf (*5*). In other marine communities where top carnivores have been removed by various agents, dramatic changes have ensued (*5, 27*).

Chthalamus anisopoma, the most frequent prey of *H. kubiniji*, has been shown to be capable of competitively excluding other species from emergent rock surfaces (*28*). *Chthalamus* abundance shows no significant changes between 1976 and 1981 at one site near Puerto Peñasco (*29*), but at another site *Chthalamus* has increased since 1978 and has remained significantly above 1978 levels (*30*). This increase in density is correlated with significant decreases in cohabiting encrusting algae and limpets (*31*). Considering the marked seasonality of northern Gulf of California populations and the difficulty of sorting out predator removal effects from impacts of other factors, it is premature to characterize these changes as responses to the removal of the top carnivore in this system.

MICHAEL L. DUNGAN
Department of Ecology and Evolutionary Biology, University of Arizona, Tucson 85721
THOMAS E. MILLER
W. K. Kellogg Biological Station, Michigan State University, Hickory Corners 49060
DONALD A. THOMSON
Department of Ecology and Evolutionary Biology, University of Arizona, Tucson

References and Notes

1. M. Nei, T. Murayama, R. Chakraborty, *Evolution* **29**, 1 (1975).
2. A. M. Cameron, in *Proceedings of the Third International Coral Reef Symposium* (Rosenstiel School of Marine and Atmospheric Science, University of Miami, Miami, Fla., 1977), p. 193–199; R. H. Chesher, *Science* **165**, 280 (1969).
3. J. Steinbeck and E. F. Ricketts, *Sea of Cortez. A Leisurely Journal of Travel and Research* (Viking, New York, 1941).
4. Personal observations of P. Vreeland, resident of Cholla Bay since 1946; P. E. Pickens and D. A. Thomson, University of Arizona Marine Sciences Program.
5. R. T. Paine, *Am. Nat.* **100**, 65 (1966).
6. L. Y. Maluf, thesis, University of Arizona, in preparation.
7. R. C. Brusca, *Common Intertidal Invertebrates of the Gulf of California* (Univ. of Arizona Press, Tucson, 1980).
8. S. A. Mackie and E. H. Boyer, *BioScience* **148**, 120 (1977); P. K. Dayton and R. T. Paine, personal communication.
9. Bacteria noted but not identified by D. V. Lightner, Environmental Research Laboratory, University of Arizona.
10. Our assessment is based on quantitative surveys during 1974–1975 [see (*6*)], on both quantitative and qualitative surveys by M.L.D. and D.A.T. from 1978 to the present, personal communications from P. K. Dayton and T. Present for the San Felipe area, from P. K. Dayton for Bahía de Los Angeles and Bahía Concepcíon, from D. W. Anderson for Bahía de Los Angeles, and from L. T. Findley for Guaymas. Specific locations of sites and details of before and after abundance of *H. kubiniji* are available from the authors.
11. M. D. Burkenroad, *Science* **103**, 684 (1946).
12. Barnacle cover was monitored regularly by M.L.D. from June 1977 to July 1978 at one site near Puerto Peñasco.
13. M. L. Dugan and D. A. Thomson, unpublished observations during 1978 to 1979 at all the sites labeled on the mainland coast (Fig. 1).
14. Subtidal species include *Pharia pyrimidata*, *Phataria unifascialis*, *Oreaster occidentalis*, and *Nidorellia armata*, all of which we have found at several sites in abundance before and after the die-off of *H. kubiniji*.
15. M. J. Sherwood, J. Word, J. Engel, P. K. Dayton, R. C Brusca, personal communications. Species showing a high incidence of disease symptoms included asteroids of the genus *Pisaster* (carnivores), *Patiria miniata* (an omnivorous asteroid), and the holothurian *Stichopus parvimensis* (a deposit feeder).
16. E. D. Haynes, *Nat. Oceanic Atmos. Adm. Tech. Memo. NMFS-OF-5* (1980).
17. R. Lasker, *Coastal Oceanogr. Climatol. News* **1**, 3 (1978); R. H. Parrish and A. Bakun, *ibid.*, p. 13; H. J. Niebauer, *ibid.* **3**, 7 (1980).
18. D. O. Duggins, *Limnol. Oceanogr.* **26**, 391 (1981).
19. Daily onshore sea surface temperature data were taken and provided by the Environmental Research Laboratory, University of Arizona. Long-term means are based on data for 1964 to 1979. The warmest 12-month consecutive period recorded was between September 1977 and August 1978.
20. NOAA Environmental Data and Information Service, *Monthly Climatic Data for the World* (National Climatic Center, Asheville, N.C., 1948 to the present).
21. D. W. Anderson, F. Gress, K. F. Mais, *Oikos*, in press.
22. D. G. Ainley, unpublished data. The Pacific Seabird Group at Point Reyes, Calif., has monitored seabird populations in the Farallon Islands since 1971; the poorest year on record in terms of the reproductive success of nine species was 1978.
23. Similar experiments were conducted by R. Abugov of the University of Arizona and J. Engel of the Catalina Marine Science Center.
24. D. H. Cushing and R. R. Dickson, *Adv. Mar. Biol.* **14**, 2 (1975); E. F. Ricketts, J. Calvin, J. W. Hedgpeth, *Between Pacific Tides* (Stanford Univ. Press, Stanford, Calif., 1968).
25. F. B. Bang and A. Lemma, *J. Insect Pathol.* **4**, 410 (1962).
26. B. A. Menge, *Oecologia* **41**, 245 (1979); J. S. Pearse, D. P. Costa, M. B. Yellin, C. R. Agegian, *Fish. Bull.* **75**, 645 (1977).
27. For example, D. O. Duggins, *Ecology* **61**, 447 (1980); J. A. Estes, N. S. Smith, J. F. Palmisano, *ibid.* **59**, 822 (1978); R. T. Paine, *ibid.* **52**, 1096 (1971).
28. M. L. Dungan, *Bull. Ecol. Soc. Am.* **62**, 69 (1981).
29. E. H. Boyer and N. P. Yensen, in *Simposium Sobre Biologia Marina III* (Universidad Autonoma de Baja California Sur, La Paz, in press).
30. M. L. Dungan and D. A. Thomson, in *ibid.*
31. M. L. Dungan, thesis, University of Arizona, in preparation.
32. We thank D. Ainley, D. Anderson, J. Brown, R. Brusca, P. Dayton, P. Delaney, J. Engel, L. Findley, T. Gibson, R. Houston, K. Nealson, R. Paine, P. Pepe, P. Pickens, T. Present, M. Sherwood, P. Vreeland, N. Yensen, and members of the Marine Sciences Group at the University of Arizona for sharing information or making helpful suggestions.

28 October 1981; revised 12 February 1982

Bismuth Vanadate: A High-Pressure, High-Temperature Crystallographic Study of the Ferroelastic-Paraelastic Transition

Abstract. *Lattice dimensions of bismuth vanadate have been determined under 37 different high-pressure or high-temperature conditions or a combination of these conditions. New high-pressure, high-temperature, single-crystal x-ray techniques were used to bracket the reversible monoclinic (ferroelastic) to tetragonal (paraelastic) transition.*

Combined high-pressure, high-temperature (*P-T*) crystallography is a powerful new technique for measuring crystal structures and stabilities at nonambient conditions. In this report we describe the application of *P-T* crystallography to the determination of a reversible phase transition.

Bismuth vanadate, $BiVO_4$, has received considerable attention since the discovery of a ferroelastic-paraelastic phase transition at 250°C by Bierlein and Sleight in 1975 (*1*). Subsequent studies of crystal structure variation with temperature (*2, 3*), Raman spectroscopy at high temperature (*4*) and high pressure (*5*), transmission electron microscopy of the domain structure (*6*), birefringence at combined high temperature and pressure (*7*), and Brillouin spectroscopy (*8*) have provided a consistent set of descriptive parameters for the transition. The high-temperature paraelastic phase has the scheelite structure (space group, $I4_1/a$; multiplicity, $Z = 4$), in which vanadium atoms are in isolated tetrahedra and bismuth atoms are coordinated by eight oxygens. This high-symmetry, undistorted form was observed above 250°C at room pressure and above 15 kbar at room temperature; thus a negative dP/dT for the transition is indicated. The low-temperature, low-pressure, ferroelastic phase is a slight distortion of the tetragonal structure to monoclinic symmetry ($I2/a$, $Z = 4$), with Bi and O atoms shifted by approximately 0.1 Å from their ideal tetragonal positions (*2*). There are two permissible orientations of the ferroelastic state, and twinning in the low-symmetry form is thus almost universal.

The transition in $BiVO_4$ is a pure displacive, reversible transformation [a "proper ferroelastic transition" in the terminology of Aizu (*9*)]. The monoclinic γ angle, therefore, gradually changes to 90° as the temperature or pressure of the second-order transition is approached. The deviation of γ from 90° is a sensitive measure of atomic displacements from their ideal tetragonal positions and is related to the order parameter of mean

0036-8075/82/0528-0991$01.00/0

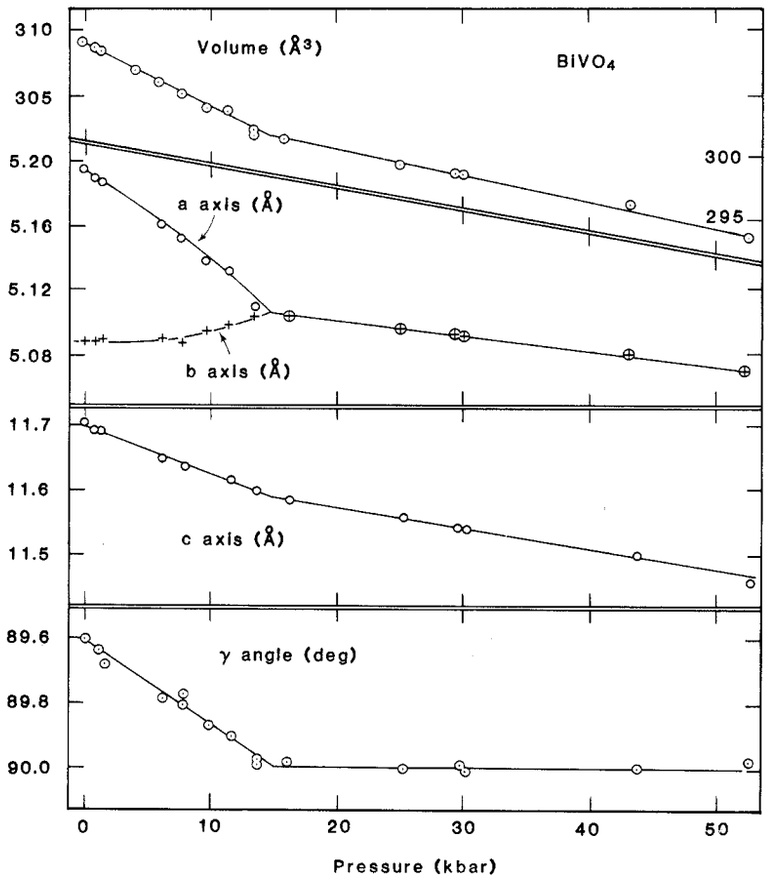

Fig. 1. Unit cell parameters of $BiVO_4$ plotted against pressure at 25°C.

field theory. All such displacements, however, are continuous and reversible, and unit cell parameters must be measured in situ under appropriate *P-T* conditions. The objective of this investigation was to apply recently developed single-crystal, *P-T*, x-ray diffraction techniques to document the variation of $BiVO_4$ unit cell parameters as a function of temperature and pressure. These data may be used to (i) define more precisely the *P-T* conditions of transition, (ii) plot the ferroelastic distortions as a function of *P* and *T* and compare them with theory (*10*), and (iii) determine equation-of-state parameters for both monoclinic and tetragonal forms of $BiVO_4$.

Synthetic single crystals of $BiVO_4$ were cut from a boule supplied by the Royal Signals and Radar Establishment (Malvern, United Kingdom). Unit cell parameters were determined on two single-crystal plates, both approximately 90 by 90 by 30 μm. One crystal plate was cut perpendicular to (001) and the other was cut perpendicular to (110). The two crystals in air yielded the same unit cell dimensions, so systematic effects due to specimen absorption are not significant.

The (110) crystal plate was then transferred to a diamond anvil pressure cell for single-crystal x-ray diffraction (*11*) in which a methanol-ethanol mixture was the hydrostatic pressure–transmitting fluid. Ruby chips 10 μm in diameter were included in the mount for pressure calibration (*12*). Unit cell parameters were measured at 16 pressures to 53 kbar. In addition, full sets of intensity data were collected at several pressures for high-pressure crystal structure determinations (*13*).

A second (110) plate was mounted with a CaF_2 calibration crystal in a *P-T* diamond anvil cell designed by Hazen and Finger (*14*) for single-crystal, x-ray diffraction studies to 450°C at pressures to 40 kbar. Temperature was controlled and measured by an external thermocouple, and pressure was deduced from the known temperature, the measured lattice constant of cubic CaF_2, and the known equation of state of CaF_2 (*15*). Unit cell parameters were determined under 21 sets of *P-T* conditions.

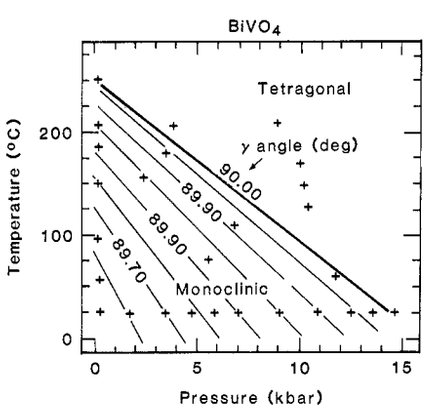

Fig. 2. Lines of constant unit cell angle γ plotted against pressure and temperature. Crosses mark *P-T* conditions of unit cell measurements.

All single-crystal, unit cell measurements were performed on an automated four-circle x-ray diffractometer with $MoK\alpha_1$ radiation (wavelength, 0.7093 Å). Each reflection was centered in eight equivalent positions after the procedure of Hamilton (*16*) to correct for systematic errors due to crystal centering and diffractometer alignment.

Unit cell parameters at 43 *P-T* conditions [including five room temperature and high-temperature unit cell measurements from (*2*) and (*3*)] were tabulated (*17*). Unit cell expansion and compression of $BiVO_4$ clearly reflect the monoclinic-tetragonal transition. Below the transition temperature the *a* axis is longer than *b*, but *a* contracts and *b* expands to an intermediate value at 250°C. Average expansion of $a + b$ is seven times greater above than below the transition, whereas expansion of the *c* axis increases by a factor of 6 from 4×10^{-6} °C^{-1} in the monoclinic form to 2.3×10^{-5} °C^{-1} in the tetragonal form. Volume thermal expansion of the monoclinic and tetragonal phases of $BiVO_4$ is 8×10^{-6} and 50×10^{-6} °C^{-1}, respectively.

Variation of unit cell parameters with pressure (Fig. 1) is, in many respects, the mirror of the temperature response. Below 15 kbar the *a* axis compresses and the *b* axis actually expands with increasing pressure. To our knowledge, this result is the first example of a crystallographic axis becoming longer with increasing hydrostatic pressure. Both the average $a + b$ axes and the *c* axis are significantly less compressible above the transition pressure than below. Volume compressibility, β, of the high-pressure tetragonal form of $BiVO_4$ ($\beta = 6.9 \times 10^{-4}$ kbar^{-1}), therefore, is nearly 60 percent less than that below the transition pressure ($\beta = 15.4 \times 10^{-4}$ kbar^{-1}). Such a large change in bulk modulus is unusual in reversible transitions.

The *P-T* cell data for $BiVO_4$ lattice dimensions may be combined on *P-T* nomograms to illustrate the systematic variations of cell parameters with pressure and temperature. Figure 2 shows lines of constant γ with negative dP/dT.

These lines are consistent with a linear *P-T* transition curve:

$$T\ (°C) = 250(\pm 3) - 15.0(\pm 8)P\ (kbar)$$

A nomogram of unit cell volume versus P and T reveals isochoric lines with positive dP/dT and with sharp breaks in slope at the transition. Positive sloping isochors could be combined with the negative sloping lines of constant γ (Fig. 2) to provide a simple single-crystal internal *P-T* standard for the range of stability of the monoclinic phase.

This study demonstrates the utility of *P-T* crystallography in the determination of phase equilibria. The *P-T* cell is a practical device for x-ray diffraction studies of single crystals to several hundred degrees centigrade and several tens of kilobars. In situ determination of lattice parameters and crystal structures at combined temperature and pressure should be especially valuable in the documentation of nonquenchable, reversible phase transitions, such as that displayed by bismuth vanadate.

R. M. HAZEN
Geophysical Laboratory,
Carnegie Institution of Washington,
Washington, D.C. 20008
J. W. E. MARIATHASAN
Clarendon Laboratory,
Parks Road,
Oxford, OX1 3PU, England

References and Notes

1. J. D. Bierlein and A. W. Sleight, *Solid State Commun.* **16**, 69 (1975).
2. W. I. F. David, A. M. Glazer, A. W. Hewat, *Phase Transitions* **1**, 155 (1979).
3. A. W. Sleight, H.-Y. Chen, A. Ferretti, D. E. Cox, *Mater. Res. Bull.* **14**, 1571 (1980).
4. A Pinczuk, G. Brown, F. H. Dacol, *Solid State Commun.* **24**, 163 (1977).
5. A. Pinczuk, B. Welber, F. H. Dacol, *ibid.* **29**, 515 (1979).
6. C. Manolikas and S. Amelinckx, *Phys. Status Solidi* **60**, 167 (1980); L. S. Wainer, R. F. Baggio, H. L. Dussel, M. A. R. Benyacar, *Ferroelectrics* **31**, 121 (1981).
7. I. G. Wood, B. Welber, W. I. F. David, A. M. Glazer, *J. Appl. Crystallogr.* **13**, 224 (1980).
8. G. Benyuan, M. Copic, H. Z. Cummins, *Phys. Rev. B* **24**, 7 (1981).
9. K. Aizu, *J. Phys. Soc. Jpn.* **27**, 2 (1969).
10. J. W. E. Mariathasan *et al.*, in preparation.
11. L. Merrill and W. A. Bassett, *Rev. Sci. Instrum.* **45**, 290 (1974); R. M. Hazen and L. W. Finger, *Carnegie Inst. Washington Yearb.* **76**, 655 (1977).
12. G. J. Piermarini, S. Block, J. D. Barnett, R. A. Forman, *J. Appl. Phys.* **46**, 2774 (1975).
13. J. W. E. Mariathasan, L. W. Finger, R. M. Hazen, in preparation.
14. R. M. Hazen and L. W. Finger, *Rev. Sci. Instrum.* **52**, 75 (1981).
15. ———, *J. Appl. Crystallogr.* **14**, 234 (1981).
16. W. Hamilton, *International Tables for X-ray Crystallography* (Kynoch, Birmingham, England, 1974), vol. 4, pp. 273–284; H. E. King and L. W. Finger, *J. Appl. Crystallogr.* **12**, 374 (1979).
17. Tabulated temperature, pressure, and unit cell data for $BiVO_4$ are available from R.M.H. on request.
18. We thank L. W. Finger, A. M. Glazer, and H. S. Yoder, Jr., for their constructive reviews of the manuscript. This research was supported in part by NSF grant EAR79-19768 and by the Science Research Council (United Kingdom).

20 January 1982; revised 22 March 1982

Stem Rust of Wheat 3300 Years Old Found in Israel

Abstract. *A fungus parasite observed on two ancient lemma fragments of wheat was identified as* Puccinia graminis. *The fragments were found in a storage jar from the Late Bronze Age excavated at Tel Batash, Israel, Uredia, hyphae, and germinating uredospores, though charred, were well preserved.*

Two rust-infected wheat lemma fragments from the Late Bronze Age II (1400 to 1200 B.C.) were found at Tel Batash on the piedmont of the Judean Mountains, Israel. The fragments were in a nearly intact storage jar that was full of wheat grains and also contained some unthreshed spikelets. The jar was excavated from a storage space located beneath wooden steps leading to the second story of a public building. It was sealed under a thick layer of charred wood and fallen bricks (*1*). Although charred, the wheat grains, as well as some ear parts, were well preserved; there was almost no damage even to the vulnerable epidermis and its hairs. The wheat belongs to the archeobotanical naked tetraploid species *Triticum parvicoccum* (*2*). Some investigators include this species in *T. turgidum* (*2, 3*).

One large longitudinal and two smaller round uredia were observed on the larger lemma fragment (Fig. 1). A large longitudinal uredium was also seen on the smaller fragment. All infestations were located on the inner concave face of the lemma. In the scanning electron microscope, various stages of spore germination, including penetration into the lemma, could be observed (Fig. 2). The characteristic ruptured epidermis of the host along with the oval echinulate uredospores (17 by 11 μm) with four equatorial germ pores (Fig. 3) enabled identification of the fungus as *Puccinia graminis* f. sp. *tritici*, the cause of stem rust of wheat (*4*). The charred uredospores are smaller and rounder than uncharred *P. graminis* f. sp. *tritici*, as is common for other archeobotanical specimens (*5*).

The delicate structures of the pustules, the hyphae, and the germinating uredospores were well protected during the

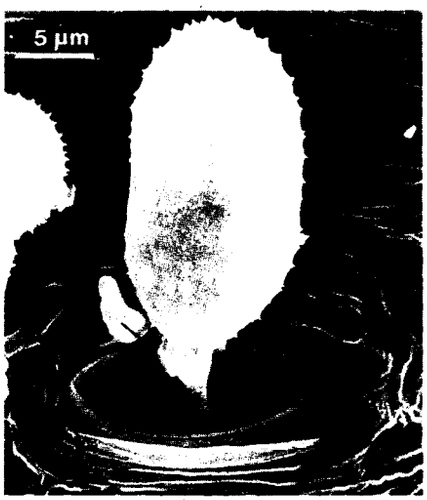

Fig. 1 (left). Pustule of *Puccinia graminis* on the inner surface of a lemma of *Triticum parvicoccum*. Fig. 2 (top right). Penetration of germinating tube into host stoma. Only remnants of the vesicle-like appressorium (arrow) are present. Fig. 3 (bottom right). Four equatorial germ pores (arrows) characteristic of *Puccinia graminis* are visible on the broken uredospore.

0036-8075/82/0528-0993$01.00/0